Click here to view PowerPoint presentation; Press Esc to exit

Studies of Ionospheric Processes in the Atmosphere and the Laboratory

T.G. Slanger
Molecular Physics Laboratory
SRI International
Menlo Park, CA 94025
U.S.A.

tom.slanger@sri.com

ABSTRACT

The ionosphere can be studied in a variety of ways – observation, modeling, and the simulation of ionospheric processes in the laboratory. Over the last several years we have carried out such studies in two ways, from ground-based observations using astronomical sky spectra, and from laboratory investigations. At altitudes above 200 km, the dominant atmospheric particles are oxygen atoms, and for any collisional studies it is always necessary to inquire as to the role of these atoms. One example is given by the oxygen red line, a ubiquitous emission in dayglow, nightglow, and aurorae, both artificial and induced. In order to understand both the intensity and the decay of this long-lived emission, one must establish the effect of collisions of the red line emitter – O(^{1}D) – with ground-state O-atoms. The conclusion reached from application of the laboratory results to atmospheric observations is that the dominant loss process at altitudes relevant to ionospheric modification experiments is in fact collisions with O(^{3}P). It follows that measuring the O(^{1}D) decay rate provides a measure of the local O-atom density. Another example comes from observation of the O_2 Atmospheric bands, which normally emit in the mesosphere, but can also be seen from the lower thermosphere. Again, it is essential to find out how the excited O_2 molecules interact with O-atoms. In this paper we demonstrate how laboratory studies are used to address these questions, how the results are applied to atmospheric issues, and also what we are being taught by the high resolution nightglow spectra accessible from astronomical systems.

1.0 INTRODUCTION

Dayglow/nightglow/auroral studies invariably involve investigations of atomic and molecular excited states. In the atmosphere, the electronic or vibrational energy of these particles is typically removed by collisions, since in the majority of cases the excited emitters are metastable with respect to radiation, so that collisional loss dominates.

There are three atmospheric colliders that are most important in this regard – O_2, N_2, and O(^{3}P) ground-state oxygen atoms. Since the former two are permanent gases, their use in the laboratory is straightforward, and investigations over the years have concentrated on making measurements with these two air components. For atmospheric chemistry at altitudes less than 90 km or so this is justifiable, because the mole fraction of O(^{3}P) is low, and O_2 and N_2 can be very efficient at removing internal energy. For higher altitudes, the situation is less clear-cut, because the O(^{3}P) density exceeds that of O_2 near 115 km, and exceeds that of N_2 near 170 km.

Slanger, T.G. (2006) Studies of Ionospheric Processes in the Atmosphere and the Laboratory. In *Characterising the Ionosphere* (pp. 1-1 – 1-12). Meeting Proceedings RTO-MP-IST-056, Paper 1. Neuilly-sur-Seine, France: RTO. Available from: http://www.rto.nato.int/abstracts.asp.

Report Documentation Page

Form Approved
OMB No. 0704-0188

1. REPORT DATE	2. REPORT TYPE	3. DATES COVERED
01 JUN 2006	**N/A**	**-**

4. TITLE AND SUBTITLE	5a. CONTRACT NUMBER
Studies of Ionospheric Processes in the Atmosphere and the Laboratory	5b. GRANT NUMBER
	5c. PROGRAM ELEMENT NUMBER
6. AUTHOR(S)	5d. PROJECT NUMBER
	5e. TASK NUMBER
	5f. WORK UNIT NUMBER
7. PERFORMING ORGANIZATION NAME(S) AND ADDRESS(ES) **Molecular Physics Laboratory SRI International Menlo Park, CA 94025 U.S.A.**	8. PERFORMING ORGANIZATION REPORT NUMBER
9. SPONSORING/MONITORING AGENCY NAME(S) AND ADDRESS(ES)	10. SPONSOR/MONITOR'S ACRONYM(S)
	11. SPONSOR/MONITOR'S REPORT NUMBER(S)

12. DISTRIBUTION/AVAILABILITY STATEMENT
Approved for public release, distribution unlimited

13. SUPPLEMENTARY NOTES
See also ADM002065., The original document contains color images.

14. ABSTRACT

15. SUBJECT TERMS

16. SECURITY CLASSIFICATION OF:			17. LIMITATION OF ABSTRACT	18. NUMBER OF PAGES	19a. NAME OF RESPONSIBLE PERSON
a. REPORT	b. ABSTRACT	c. THIS PAGE			
unclassified	**unclassified**	**unclassified**	**UU**	**32**	

Thus, when O_2 is a more important collider than N_2, often the case, then at the relatively low altitude of 115 km, it is necessary to know the relative collisional efficiencies of $O(^3P)$ and O_2. In any case, above 170 km, where there is little O_2, information on the relative effects of $O(^3P)$ and N_2 is needed.

Because of the difficulty of generating $O(^3P)$ in the laboratory in sufficient quantities to be a competitive collider with O_2 and N_2, there has been a tendency to ignore the possible atmospheric role of $O(^3P)$ in collisions, and accept the results of calculations or the output of models. However, there is no substitute for unambiguous experiments, and we have explored O-atom quenching parameters in a variety of systems. These include effects on $O(^1D)$ [1], of relevance to HAARP observations, and on vibrationally-excited levels of the O_2 ground state [2] and the $b^1\Sigma_g^+$ excited state [3].

Synergy with the laboratory work is encountered by analysis of the high-quality nightglow sky spectra that we have been obtaining from astronomical sites with large telescopes. Most relevant to ionospheric investigations are the observations of emission from the v = 1 level of the $O_2(b^1\Sigma_g^+)$ state [4]. Under high-excitation conditions this radiation is emitted primarily from the lower thermosphere, as a consequence of energy transfer from $O(^1D)$, and detection of the radiation leads to a measure of the local temperature, far higher than in the mesosphere where $b^1\Sigma_g^+$ emission normally originates. From space, this high altitude emission can be interpreted in terms of the local O_2 and O-atom densities.

A sky spectrum is the correction that astronomers need when carrying out spectral analysis of an astrophysical object [5]. It is the sum of all extraneous emissions, a large component of which is the terrestrial nightglow. The sky spectrum is obtained from the portion of the spectrograph slit that is not occupied by the astronomical target. This spectrum is then digitally subtracted from the object spectrum, and either archived or discarded.

Telescopes with large echelle spectrometers and CCD detection generate high resolution data, with broad spectral coverage and high sensitivity. As an example, the HIRES echelle spectrometer on the Keck I telescope in Hawai'i is typically operated at a resolution of 40,000, with a spectral range of 200 nm. Data collection is normally carried out for a period of 50-minutes, so that temporal fluctuations in the nightglow on a much shorter scale cannot be followed. The telescope moves across the sky at the appropriate rate to track a given object, and astronomers view 4-6 objects in the course of a night, often in different portions of the sky.

2.0 DISCUSSION

An example of ionospheric emission viewed from the ground comes from observation of the $O_2(b\text{-}X)$ 1-1 Atmospheric band [4]. The Atmospheric band system is normally associated with the mesopause region, where $O_2(b^1\Sigma_g^+)$ is one of the several O_2 electronic states generated by O-atom recombination. However, b(v = 1) emission produced this way is generally quite weak, because it is rapidly quenched by O_2 collisions.

There is another source of b(v = 1) emission, the energy transfer reaction between $O(^1D)$ and O_2, which produces both v = 1 and v = 0. In the early evening, when $O(^1D)$ densities are still high from solar insolation, this energy transfer can occur, and the signature which demonstrates that the source is in the ionosphere and not in the mesosphere is the rotational temperature of the emitter. Because the electronic state is metastable with respect to radiation, $O_2(b)$ molecules suffer many collisions prior to radiating, and so the rotational distribution reflects the local kinetic temperature.

Figure 1 shows an example of ionospheric *b-X* 1-1 emission, and the enhanced intensity and temperature found when the emission comes from thermospheric altitudes. We find that there is always at least a small high-altitude component, but Figure 1 demonstrates that sometimes, particularly near solar maximum, it represents almost all of the radiation. We have found that the atmosphere contains a large range of $O_2(b)$ vibrationally-excited levels, up to v = 15 [6], but only the v = 0,1 levels originate in the ionosphere. Furthermore, the v = 0 emission in the 0-0 band (the Fraunhofer A-band in absorption) cannot be seen from the ground. Figure 1 also shows a DIATOM spectral simulation of the 1-1 band, which is best modeled with a temperature of 900 K, far above the typical mesopause temperature near 200 K.

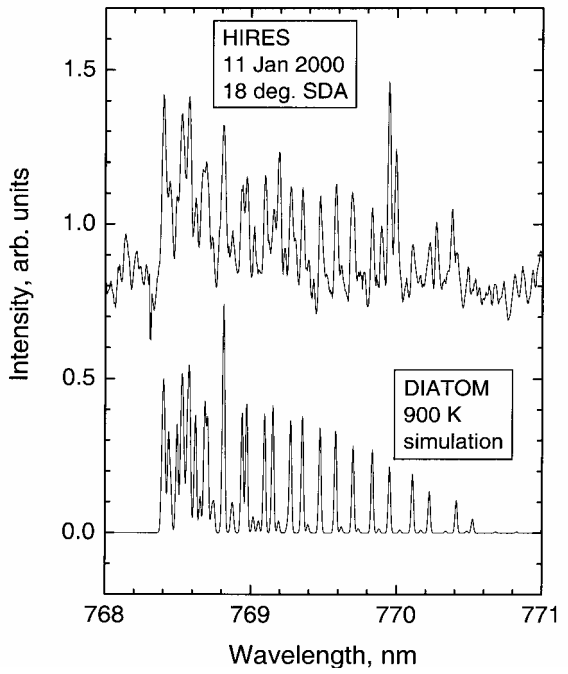

Figure 1: Ionospheric emission in the $O_2(b\text{-}X)$ 1-1 band, and a 900 K DIATOM simulation [4]

From space, both the 0-0 and 1-1 bands can be seen, and the ratio of the two is very dependent on altitude. The reason for this is clear; the v = 0 level is totally unquenched in the thermosphere, while quenching of the v = 1 level by O_2 is fast [7]. Moreover, we have recently demonstrated that O-atom quenching of v = 1 is also important [8]. In Figure 2 the three loss processes – radiation, O_2 quenching, and O-atom quenching – are given for $O_2(b, v = 1)$ [9].

With this information, a limb measurement of the emission ratio in the 0-0 and 1-1 bands defines the $O(^3P)$ + O_2 density at the observed altitude. Still, one further piece of information is required – the nascent ratio of v = 0,1 generated by the $O(^1D)$ + O_2 transfer. This has also been addressed in the Molecular Physics Laboratory. The measurement was attempted a number of years ago, and at that time it was concluded that the energy transfer products were 40% v = 1 and 60% v = 0 [10]. The experiment has recently been repeated and improved upon, and it now appears that the v = 1 yield is 77% [*Pejakovic et al.*, MS in preparation].

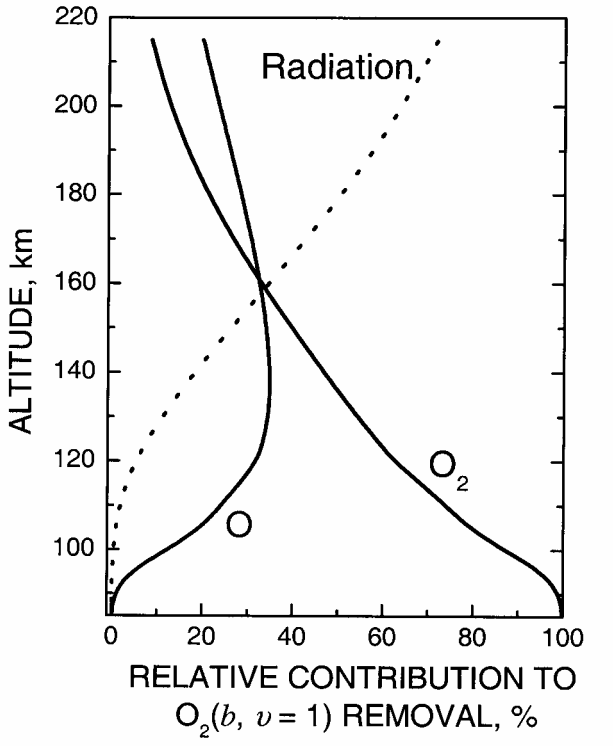

Figure 2: The percentage of $O_2(b, v = 1)$ removed by the three loss processes – radiation, O_2 quenching, and O-atom quenching – as a function of altitude [9].

The emissions of the *b*-*X* 0-0 and 1-1 bands have been measured from the space shuttle, as shown in Figure 3. This plot shows the two bands in a limb view, measured over a range of altitudes, from 142 km at the top to 166 km at the bottom. With decreasing altitude the 0-0 band becomes stronger, both absolutely and with respect to the 1-1 band, the latter effect being due to the quenching effect of O_2 and $O(^3P)$ on the $b(v = 1)$ level, collisions converting $b(v = 1)$ to $b(v = 0)$. The modeled (dashed) profile matches the lowest altitude spectrum, and is calculated for a temperature of 600 K, a resolution of 3 nm, and with a 70:30 ratio for the 0-0 and 1-1 bands, although the nascent ratio is 23:77. It is therefore possible to make limb measurements from space platforms that can be related to the thermospheric O-atom profile.

Although the $O(^1D) + O_2$ energy transfer process results in emissions readily discernible from space and from the ground, in the thermosphere above 200 km the dominant collider is $O(^3P)$, and the question of $O(^1D) + O(^3P)$ interaction has been discussed and debated for many years [11,12,13,14]. On the other hand, the results of ionospheric heating experiments have been interpreted in terms of $O(^1D)$ quenching by N_2 alone, with a minor contribution by O_2 [15,16,17,18]. It has only been relatively recently that O-atom quenching has been seriously considered as an important process in the heating experiments [19,20].

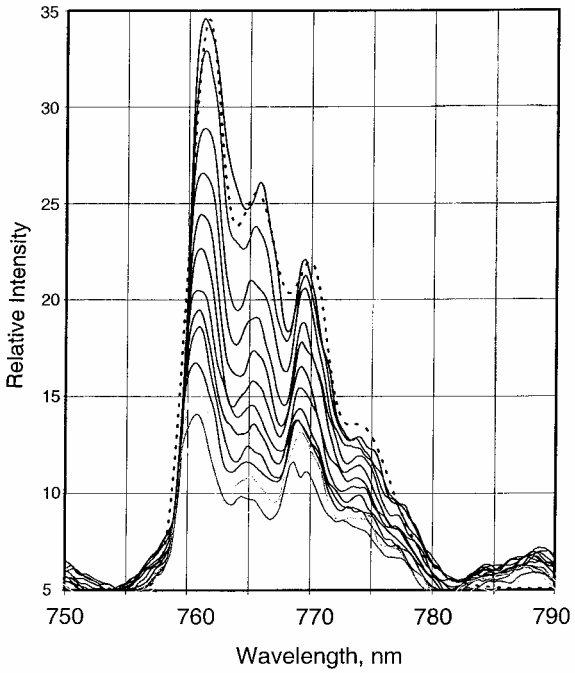

Figure 3: Series of spectra taken in the region of the O_2 Atmospheric 0-0 and 1-1 bands (Arizona GLO experiment on the space shuttle, courtesy of Lyle Broadfoot). The altitude range covered is 142-166 km (top to bottom). With increasing altitude, the 1-1 band intensity approaches that of the 0-0 band. The dashed line is a DIATOM simulation of the two bands in the lowest altitude spectrum, at a resolution of 3 nm and a temperature of 600 K. The modeled intensities are 70% 0-0 and 30% 1-1

If the $O(^1D) + O(^3P)$ reaction is important for $O(^1D)$ collisional removal, then with knowledge of the rate coefficient (k_o) for the reaction, the atmospheric decay time of the red line leads directly to an O-atom density. In Table 1 are presented data deduced over the years for the $O(^1D) + O(^3P)$ rate coefficient, from theory, experiment, and atmospheric observations. There is a single unpublished laboratory measurement of our own, where a negative result from an experiment led to the conclusion that the rate coefficient had to be just one half that for the $O(^1D) + O_2$ reaction, thus having a value of 2×10^{-11} cm^3 s^{-1}.

A laboratory measurement of k_o is difficult because one needs to make $O(^3P)$ a dominant quencher, yet most other system components are also effective $O(^1D)$ quenchers. Our solution has been to use F_2 laser (157 nm) photodissociation of O_2 as the source, where an intense pulse of light leaves a reaction volume composed of equal amounts of $O(^1D)$ and $O(^3P)$ [1]. The rapid $O(^1D)$ disappearance then corresponds to a situation where $O(^1D)$ decays in an environment of only O-atoms - $O(^3P)$ and $O(^1D)$. By carrying out experiments in which the O_2 density and the laser power are varied, it is possible to extract a value for k_o. Figure 4 shows the data, a plot of $O(^1D)$ decay constant vs O_2 density. Because the O_2 is bleached by the laser pulse in the interaction volume, the O-atom density is twice the initial O_2 density [1]. The slope of the line is the rate coefficient, which at 300 K has a value of $(2.2 \pm 0.6) \times 10^{-11}$ cm^3 s^{-1}, consistent with the conclusion reached from our much earlier experiment.

Table 1: Estimates of the Rate Coefficient for $O(^1D) + O(^3P) \rightarrow O(^3P) + O(^3P)$

Source	Rate coefficient ($cm^3\ s^{-1} \times 10^{12}$)	Method
[11]	8.0 ± 7.0	calculation
[14]	6-11 (300 K) 8-13 (1000 K)	calculation
[12]	"reaction not required to explain 6300 Å airglow data"	modeling
[13]	0-2.8 Average, 0.9	atmospheric observation
Slanger (unpublished results, 1985)	20	experiment
[1]	22 ± 0.6 (300 K, 2σ)	experiment

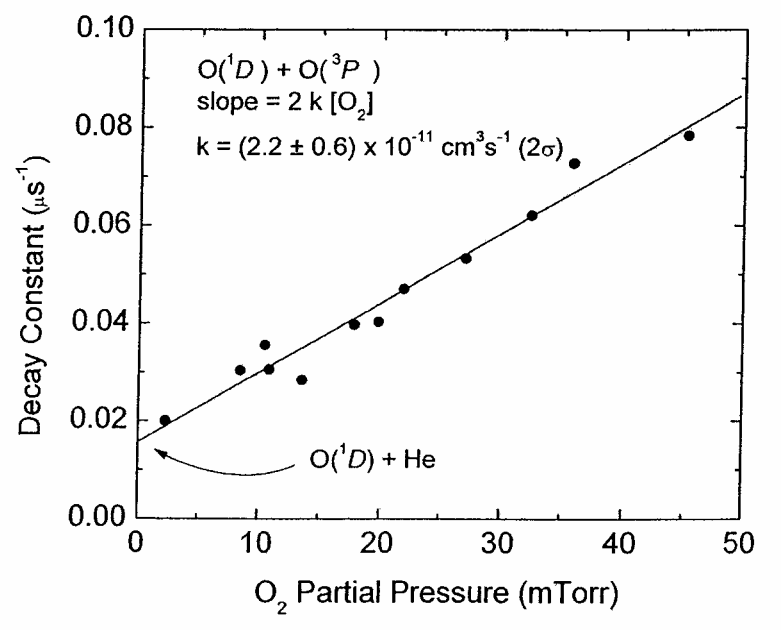

Figure 4: The $O(^1D)$ decay rate vs $[O(^3P)]$ [1]

Thus, $O(^3P)$ is an efficient quencher of $O(^1D)$, the rate coefficient being essentially the same as that for N_2. Using the 300 K value and the Jacchia 1977 model for the atmospheric composition, we are then able to construct the plot shown in Figure 5, where the fractions of total $O(^1D)$ loss by radiation and the three quenchers – $O(^3P)$, N_2, and O_2 – are given. In the region of most interest to current ionospheric heating experiments, 250-300 km, it is evident that $O(^3P)$ is the important collider, contrary to earlier assumptions [15,16,17,18]. It then follows that a measurement of the $O(^1D)$ decay time as a function of altitude over the above range provides an O-atom profile.

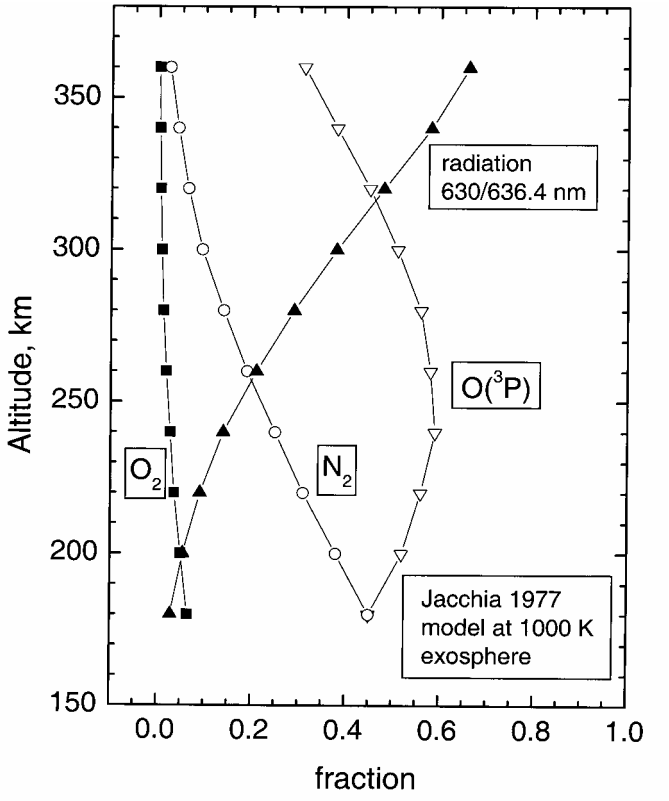

Figure 5: The fractions of total $O(^1D)$ loss by radiation and the three quenchers – $O(^3P)$, N_2, and O_2 - as a function of altitude.

We can then use lifetime and altitude data collected over the years from various facilities to determine whether a consistent picture emerges. In Table 2 we list observed lifetimes and altitudes that have been reported [18,20,21]. The O-atom density in the last column comes from the expression

$$[O(^3P)] = [\tau^{-1} - \tau_r^{-1} - kN_2\,[N_2]]/k_{O(3P)}$$

τ^{-1} is the reported decay rate in s^{-1}, $k_{O(3P)}$ is 2.2×10^{-11} cm^3 s^{-1}, k_{N2} is 2.0×10^{-11} cm^3 s^{-1}, $[N_2]$ is from MSIS-86 for the given conditions, and τ_r^{-1}, the radiative rate, is taken as 0.0090 s^{-1} [22,23]. It is obviously desirable to make laboratory measurements at thermospheric temperatures, but calculations suggest that there is only a small increase in rate coefficient with increasing temperature [14]. In the column of observed lifetimes in Table 2, the figures in parentheses are the necessary lifetimes to make the deduced O-atom density equal to that given in the MSIS-86 model.

Table 2: Ionospheric Modification Data for Three Sites, and Comparison of Modeled and Deduced $O(^3P)$ Densities

Site	Date	Source	Lifetime (sec)	Altitude (km)	Deduced $[O(^3P)]$ ($cm^{-3} \times 10^{-9}$)	MSIS-86 $[O(^3P)]$ ($cm^{-3} \times 10^{-9}$)
Platteville 49N, 105W	10/30/70 0132 UT	[18]	12.7 (9.9)	225	2.0	3.06
	10/30/70 0130 UT		13.1 (9.9)	225	1.9	3.06
SURA 56N, 46E	3/24/95 1830 UT	[20]	29.4 (33)	260	0.94	.077
	3/24/95 1737 UT		43.4 (44)	278	0.54	0.53
HAARP 62N, 145W	3/20/04 0617 UT	[21]	54 (44)	290	0.33	0.54

In Table 3, comparison is made of the difference between the deduced and modeled $O(^3P)$ densities (the last two columns in Table 2), and the N_2 densities (deduced and modeled) that result from assuming that all quenching is by N_2 [17] or that $O(^1D)$ quenching by $O(^3P)$ is inconsequential [12]. We see that the discrepancy between deduced $O(^3P)$ concentrations and MSIS-86 is relatively small when quenching by $O(^3P)$ is dominant, but is a factor of 2.7-6.5 when only N_2 is considered. In retrospect, this result was foreshadowed by the conclusion that if N_2 is the only quencher, then the N_2 rate coefficient for $O(^1D)$ quenching is 9×10^{-11} cm^3 s^{-1} [17], whereas it is now well-known that the true value is close to 2×10^{-11} cm^3 s^{-1} [24].

Table 3. Determination of deduced:modeled $O(^3P)$ and deduced:modeled N_2 for a) $O(^1D)$ collisional loss is primarily due to $O(^3P)$, and b) $O(^1D)$ collisional loss is entirely due to N_2.

Site	$[O(^3P)]$ from $O(^1D)$ quenching by $O(^3P)$, Deduced/MSIS	$[N_2]$ (cm^{-3}) deduced	$[N_2]$ (cm^{-3}) MSIS-86	$[N_2]$ from N_2 quenching of $O(^1D)$. Deduced/MSIS
Platteville	0.65	3.5E9	1.26E9	2.8
	0.62	3.4E9	1.26E9	2.7
SURA	1.23	1.3E9	2.07E8	6.3
	1.03	7.0E8	1.08E8	6.5
HAARP	0.62	5.0E8	1.09E8	4.6

Contrary to the analysis of Link and Cogger [12], where it was concluded that the $O(^1D) + O(^3P)$ reaction was unnecessary to explain thermospheric $O(^1D)$ photochemistry, it now appears that it is the most important loss process for $O(^1D)$ over a large altitude range, from 180 km below which N_2 quenching becomes dominant, to 315 km, above which radiation takes over. One should take note of the fact that relaxation of $O(^1D)$ by $O(^3P)$ results in production of two atoms with a translation energy of 1-eV each. Deactivation by N_2, on the other hand, leads ultimately to generation of $N_2(v = 1)$, with an internal energy of 0.29 eV. The subsequent degradation of these two forms of energy may have different consequences.

In addition to the studies described here, the availability of astronomical sky spectra has opened up a major new area of atmospheric investigations, and a variety of other lines of research have been pursued. These include unique studies of the sodium nightglow [25], discovery of a new O_2 band system [27], exploration of radiative recombination in O^+ [27], precise measurements of line ratio intensities in $O(^1D)$ and $N(^2D)$ [28,29], identifications of 2800 atomic and molecular lines in the nightglow [30], and detailed studies of OH spectroscopy [31]. Because we have been limited to observations in tropical regions – where the large telescopes are sited – we have proposed to NSF that the construction of a portable echelle spectrograph with the capabilities of the astronomical systems would be a huge benefit to the aeronomical community. If this is funded, the first location of CESAR (Compact Echelle Spectrograph for Aeronomical Research) would be in Alaska, and the high speed, high resolution, and broad spectral coverage of such a system would provide a new dimension to auroral research.

3.0 CONCLUSION

It has been demonstrated, through laboratory experiments, modeling, and atmospheric observations, that the effect of $O(^3P)$ as a collider is often of critical importance in understanding optical emissions in the thermosphere. In the case of the $O(^1D\text{-}^3P)$ red lines, it now appears that quenching of $O(^1D)$ by $O(^3P)$ is the dominant process for altitudes above 180 km, only being exceeded in loss efficiency above 300 km by the radiative decay. It follows that over at least this altitude range, the local $O(^3P)$ density can be extracted from observations of the red line decay that follows ionospheric heating experiments. Such experiments carried out at Platteville, SURA, and HAARP show good correspondence between $O(^3P)$ densities deduced in this manner and the MSIS-86 model.

A further demonstration of the effect of O-atoms in the ionosphere comes from space-based observation of the O_2 Atmospheric 0-0 and 1-1 bands, where emission from the $v = 1$ level is sensitive to the O-atom density. Ground-based observation of the 1-1 band is complementary, and rotational distributions at early evening times probe the local kinetic temperature, which is often seen to lie in the 700-900 K range, far above the 200 K temperature typical of mesospheric O_2 Atmospheric band emission. Observations of this type are immensely aided by accessibility to the sky spectra that are generated by the echelle spectrographs at major telescope sites.

4.0 ACKNOWLEDGMENTS

This work was supported by the NSF Aeronomy and NASA ITM programs. This paper includes data based on observations made at the W. M. Keck Observatory, which is operated jointly by the California Institute of Technology and the University of California.

5.0 REFERENCES

[1] Closser, K.D., D.A. Pejaković, and K.S. Kalogerakis, O(^{1}D) relaxation by O(^{3}P), in AGU Fall meeting, paper SA11A-0215, San Francisco, CA, 2005.

[2] Kalogerakis, K.S., T.G. Slanger, and R.A. Copeland, Vibrational energy transfer in $O_2(X^3\Sigma_g^-$, v = 2, 3) + O_2 collisions at 330 K, Journal of Chemical Physics, 123, 044309, 2005.

[3] Kalogerakis, K.S., R.A. Copeland, and T.G. Slanger, Collisional removal of $O_2(b^1\Sigma_g^+$, v = 2,3), Journal of Chemical Physics, 116, 4877-4885, 2002.

[4] Slanger, T.G., P.C. Cosby, and D.L. Huestis, Ground-based observation of high-altitude high-temperature emission in the O_2 Atmospheric band nightglow, Journal of Geophysical Research, 108 (A7), 10.1029/2003JA009885, 2003.

[5] Slanger, T.G., and D.E. Osterbrock, Aeronomy-astronomy collaboration focuses on nighttime terrestrial atmosphere, EOS, Transactions of the American Geophysical Union, 79, 149, 150, 154, 1998.

[6] Slanger, T.G., P.C. Cosby, D.L. Huestis, and D.E. Osterbrock, Vibrational level distribution of $O_2(b^1\Sigma_g^+$, v = 0-15) in the mesosphere and lower thermosphere region, Journal of Geophysical Research, 105, 20557-20564, 2000.

[7] Hwang, E.S., A. Bergman, R.A. Copeland, and T.G. Slanger, Temperature dependence of the collisional removal of $O_2(b^1\Sigma_g^+$, v = 1 and 2) at 110 - 260 K, and atmospheric applications, Journal of Chemical Physics, 110, 18-24, 1999.

[8] Pejakovic, D.A., R.A. Copeland, T.G. Slanger, and K.S. Kalogerakis, Collisional removal of $O_2(b^1\Sigma_g^+$, v = 1) by O(^{3}P), Chemical Physics Letters, 405, 372-377, 2005.

[9] Pejakovic, D.A., E.R. Wouters, K.E. Phillips, T.G. Slanger, R.A. Copeland, and K.S. Kalogerakis, Collisional removal of $O_2(b^1\Sigma_g^+$, v = 1) by O_2 at thermospheric temperatures, Journal of Geophysical Research, 110, A03308, doiI:10,1029/2004JA010860, 2005.

[10] Lee, L.C., and T.G. Slanger, Observations of O(^{1}D - ^{3}P) and $O_2(b^1\Sigma_g^+ - X^3\Sigma_g^-)$ following O_2 photodissociation, Journal of Chemical Physics, 69, 4053-4060, 1978.

[11] Abreu, V.J., J.H. Yee, S.C. Solomon, and A. Dalgarno, The quenching rate of O(^{1}D) by O(^{3}P), Planet. Space Sci., 34, 1143-46, 1986.

[12] Link, R., and L.L. Cogger, A reexamination of the O I 6300-Å nightglow, J. Geophys. Res., 93 (A9), 9883-9892, 1988.

[13] Sobral, J.H.A., H. Takahashi, M.A. Abdu, P. Muralikrishna, Y. Sahai, and C.J. Zamlutti, O(^{1}S) and O(^{1}D) quantum yields from rocket measurements of electron densities and 557.7 and 630.0 nm emissions in the nocturnal F-region, Planetary Space Science, 40, 607-620, 1992.

[14] Yee, J.-H., S.L. Guberman, and A. Dalgarno, Collisional quenching of O(^{1}D) by O(^{3}P), Planet. Space Sci., 38, 647-652, 1990.

[15] Bernhardt, P.A., L.M. Duncan, and C.A. Tepley, Artificial airglow excited by high-power radio waves, Science, 242, 1022-1027, 1988.

[16] Bernhardt, P.A., C.A. Tepley, and L.M. Duncan, Airglow enhancement associated with plasma cavities formed during ionospheric heating experiments, J. Geophys. Res., 94 (A7), 9071-9092, 1989.

[17] Hernandez, G., Determination of the quenching of O(^{1}D) by molecular nitrogen using the ionospheric modification experiment, J. Geophys. Res., 77, 3625-3629, 1972.

[18] Sipler, D.P., and M.A. Biondi, Measurements of O(^{1}D) quenching rates in the F region, J. Geophys. Res., 77, 6202-6212, 1972.

[19] Melendez-Alvira, D.J., D.G. Torr, P.G. Richards, W.R. Swift, M.R. Torr, T. Baldridge, and H. Rassoul, Sensitivity of the 6300 Å airglow to neutral composition., J. Geophys. Res., 100 (A5), 7839-7853, 1995.

[20] Bernhardt, P.A., M. Wong, J.D. Huba, B.G. Fejer, L.S. Wagner, J.A. Goldstein, C.A. Selcher, V.L. Frolov, and E.N. Sergeev, Optical remote sensing of the thermosphere with HF pumped artificial airglow, J. Geophys. Res., 105 (A5), 10657-10671, 2000.

[21] Djuth, F.T., T.R. Pedersen, E.A. Gerken, P.A. Bernhardt, C.A. Selcher, W.A. Bristow, and M.J. Kosch, Ionospheric modification at twice the electron cyclotron frequency, Phys. Rev. Letters, 94 (12), 125001 1-4, 2005.

[22] Fischer, C.F., and H. Saha, Multiconfiguration Hartree-Fock results with Breit-Pauli corrections for forbidden transitions in the 2p(4) configuration, Physical Review A, 28, 3169-3178, 1983.

[23] Storey, P.J., and C.P. Zeippen, Theoretical values for the [OIII] 5007/4959 line-intensity ratio and homologous cases, Mon. Not. R. Astron. Soc., 312, 813-816, 2000.

[24] Sander, S.P., R.R. Friedl, D.M. Golden, M.J. Kurylo, R.E. Huie, V.L. Orkin, G.K. Moortgat, A.R. Ravishankara, C.E. Kolb, M.J. Molina, and B.J. Finlayson-Pitts, Chemical kinetics and photochemical data for use in stratospheric modeling, Evaluation number 14, National Aeronautics and Space Administration, Jet Propulsion Laboratory, 2003.

[25] Slanger, T.G., P.C. Cosby, D.L. Huestis, A. Sais-Lopez, B.J. Murray, D.A. O'Sullivan, J.M.C. Plane, C. Allende-Prieto, J. Martin-Torres, and P. Jenniskens, Variability of the mesospheric nightglow Na(D_2/D_1) ratio, Journal of Geophysical Research, 110, D23302, doi:10.1029/2005JD006078., 2005.

[26] Slanger, T.G., P.C. Cosby, and D.L. Huestis, A new O_2 band system: The $c^1\Sigma_u^-$ - $b^1\Sigma_g^+$ transition in the terrestrial nightglow, Journal of Geophysical Research, 108 (A2), 1089, 2003.

[27] Slanger, T.G., D.L. Huestis, P.C. Cosby, and R.R. Meier., Oxygen atom Rydberg emission in the equatorial ionosphere from radiative recombination, Journal of Geophysical Research, 109 (A10), 10309, 2004.

[28] Sharpee, B.D., and T.G. Slanger, The O($^1D_2$-$^3P_{2,1,0}$) 630.0, 636.4, and 639.2 nm forbidden emission line intensity ratios measured in the terrestrial nightglow, Journal of Physical Chemistry A, in press, 2006.

[29] Sharpee, B.D., T.G. Slanger, P.C. Cosby, and D.L. Huestis, The N($^2D^o$-$^4S^o$) 520 nm forbidden doublet in the nightglow: an experimental test of the theoretical intensity ratio, Geophysical Research Letters, 32, L12106, doi.1029/2005GL023044, 2005.

[30] Sharpee, B.D., P.C. Cosby, D.L. Huestis, T.G. Slanger, and R. Hanuschik, High-resolution telluric emission line atlas from UVES/VLT and HIRES Keck/I: positions, intensities, and assignments for 2810 lines at 314-1043 nm, Journal of Geophysical Research, submitted, 2006.

[31] Cosby, P.C., and T.G. Slanger, OH spectroscopy and dynamics investigated with astronomical sky spectra, Canadian Journal of Physics, submitted, 2006.

Studies of Ionospheric Processes in the Atmosphere and the Laboratory

T. G. Slanger
Molecular Physics Laboratory
SRI International
Menlo Park, CA 94025

URSI/NATO Conference; Fairbanks, Alaska,
12-16 June 2006

OUTLINE

1) Characteristics of sky spectra
2) O_2 Atmospheric band emission; differentiating mesospheric and thermospheric sources
3) Cold and hot $O_2(b)$ v = 1 emission
4) Ionospheric loss of b(v = 1)
5) Ionospheric modification - $O(^1D)$ decays
6) $O(^1D) + O(^3P)$ interaction data
7) Observed $O(^1D)$ lifetimes
8) Derived and modeled O-atom densities
9) Conclusions

Keck I and Keck II telescopes, Mauna Kea

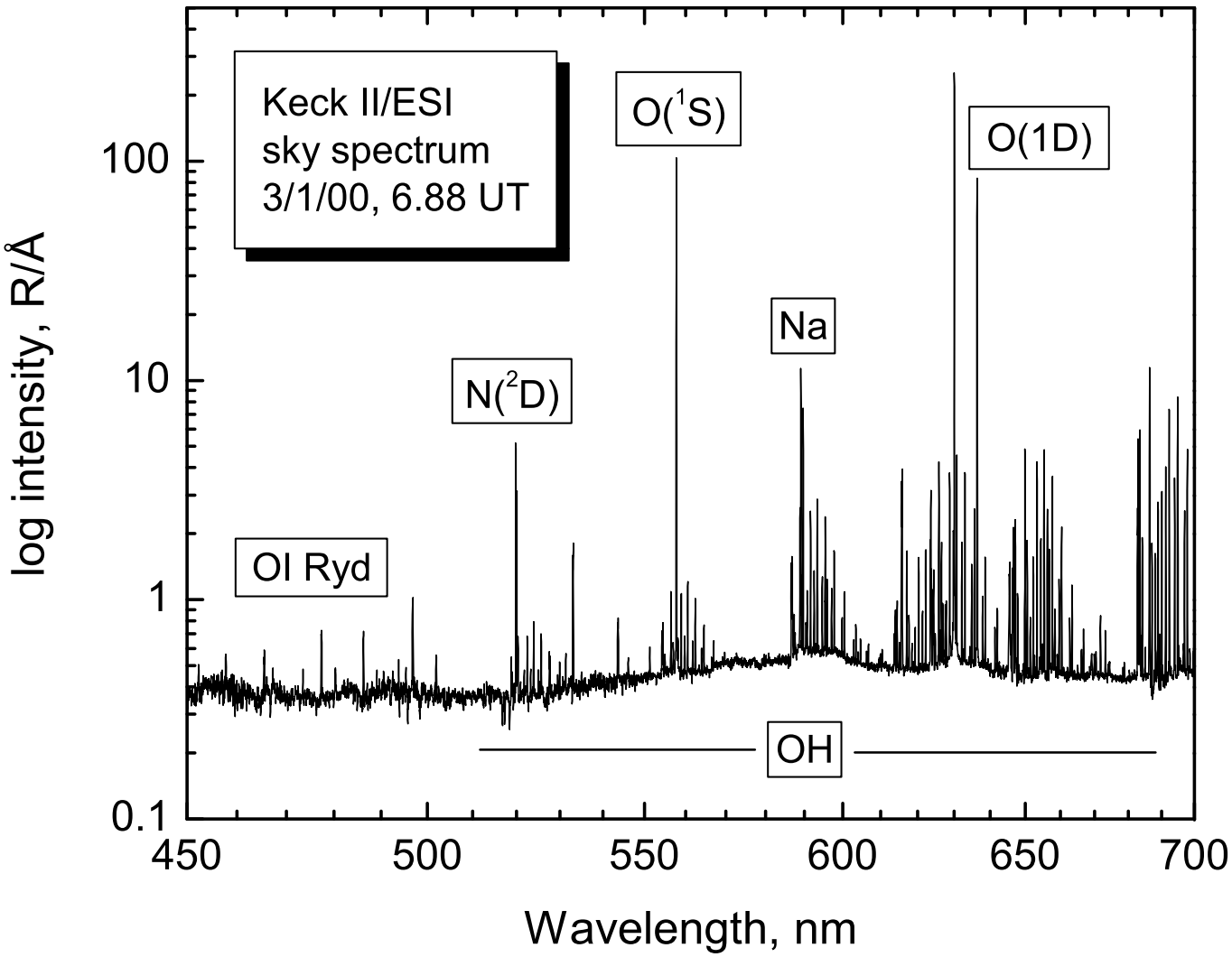
Keck II/ESI
sky spectrum
3/1/00, 6.88 UT
O(1S)
O(1D)
Na
N(2D)
OI Ryd
OH
log intensity, R/Å
100
10
1
0.1
450
500
550
600
650
700
Wavelength, nm

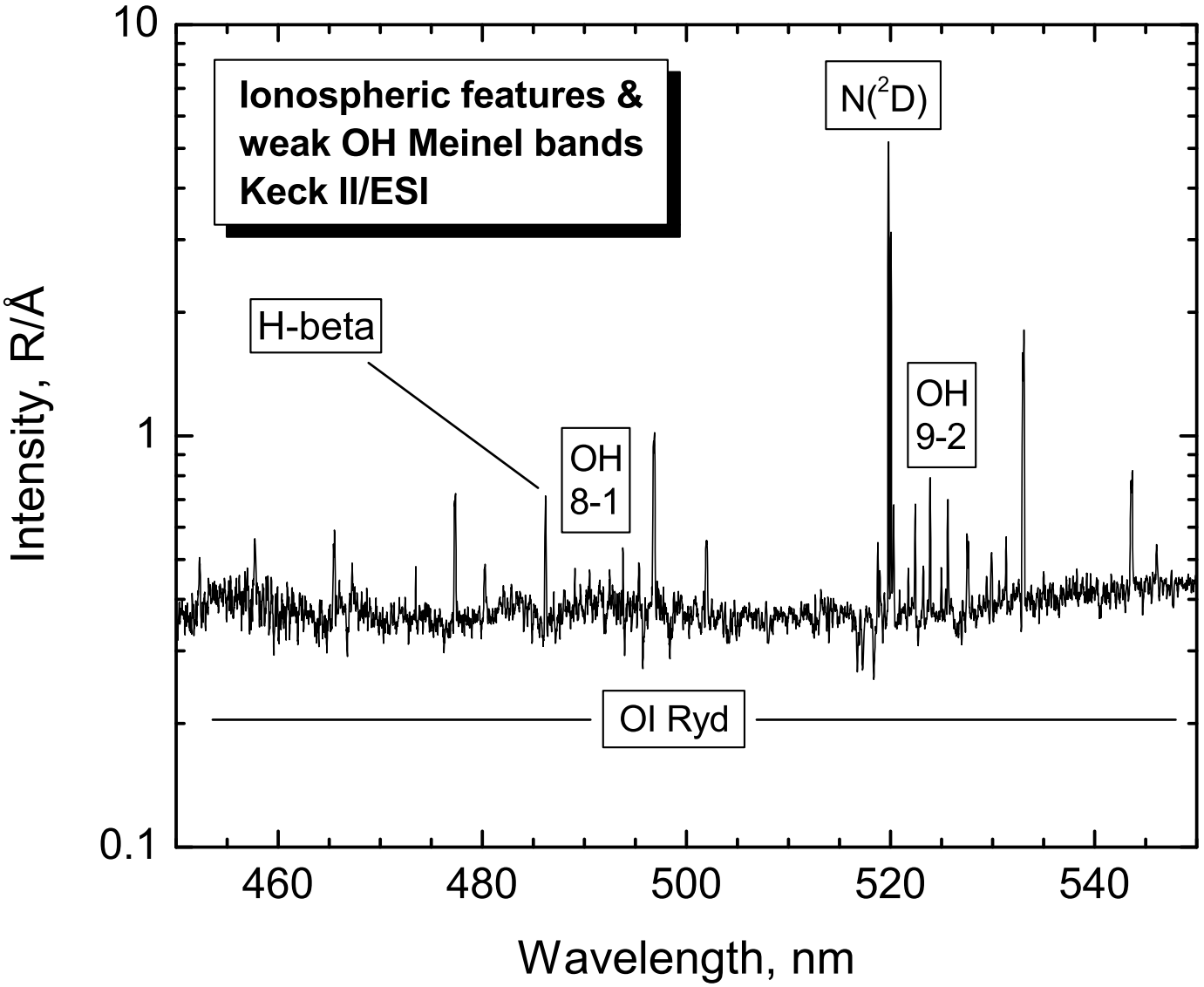
Ionospheric features &
weak OH Meinel bands
Keck II/ESI
N(2D)
H-beta
OH
8-1
OH
9-2
OI Ryd
10
1
0.1
Intensity, R/Å
460
480
500
520
540
Wavelength, nm

TGS1

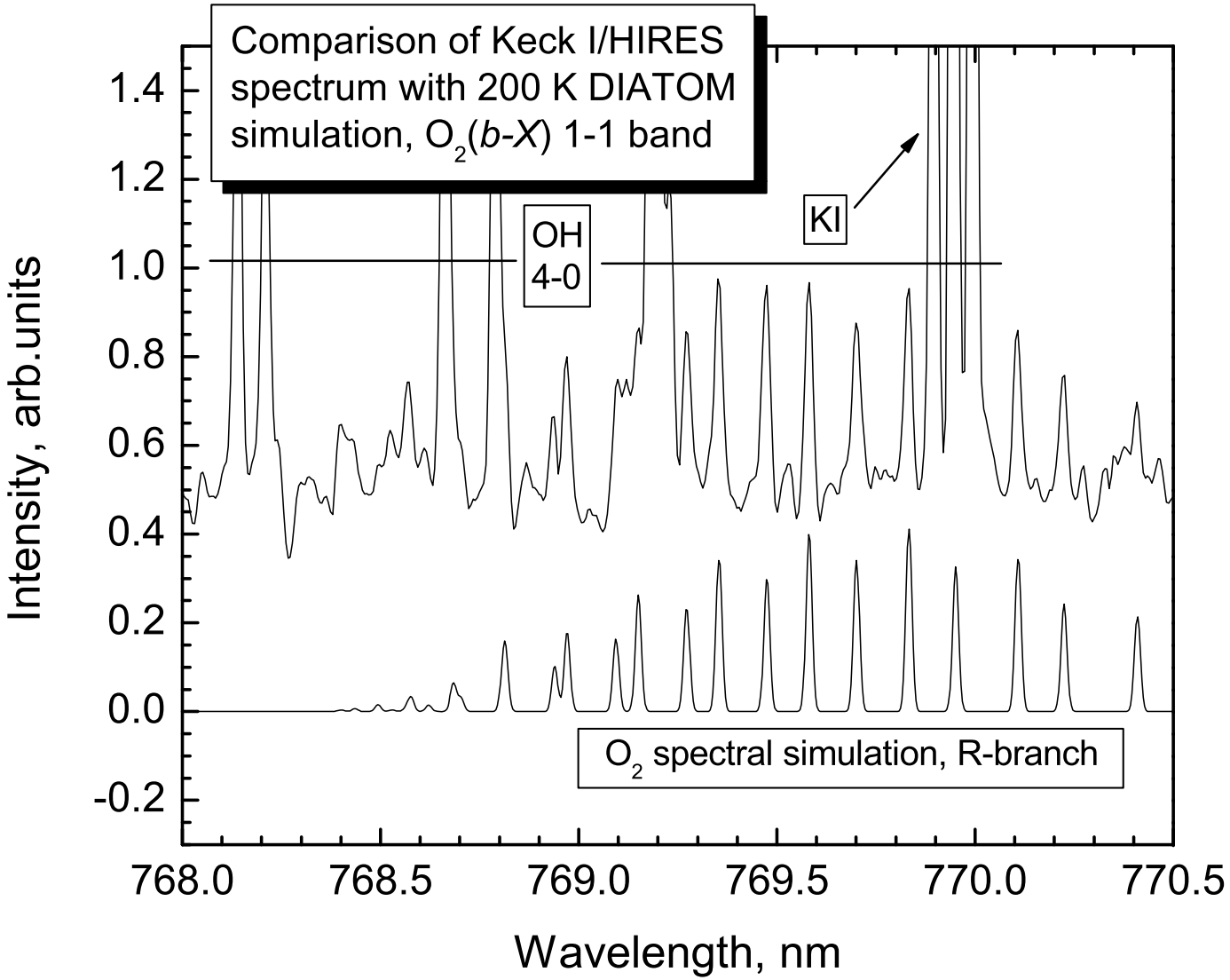
Comparison of Keck I/HIRES spectrum with 200 K DIATOM simulation, O2(b-X) 1-1 band
OH 4-0
KI
O2 spectral simulation, R-branch
Intensity, arb.units
Wavelength, nm
1.4
1.2
1.0
0.8
0.6
0.4
0.2
0.0
-0.2
768.0
768.5
769.0
769.5
770.0
770.5

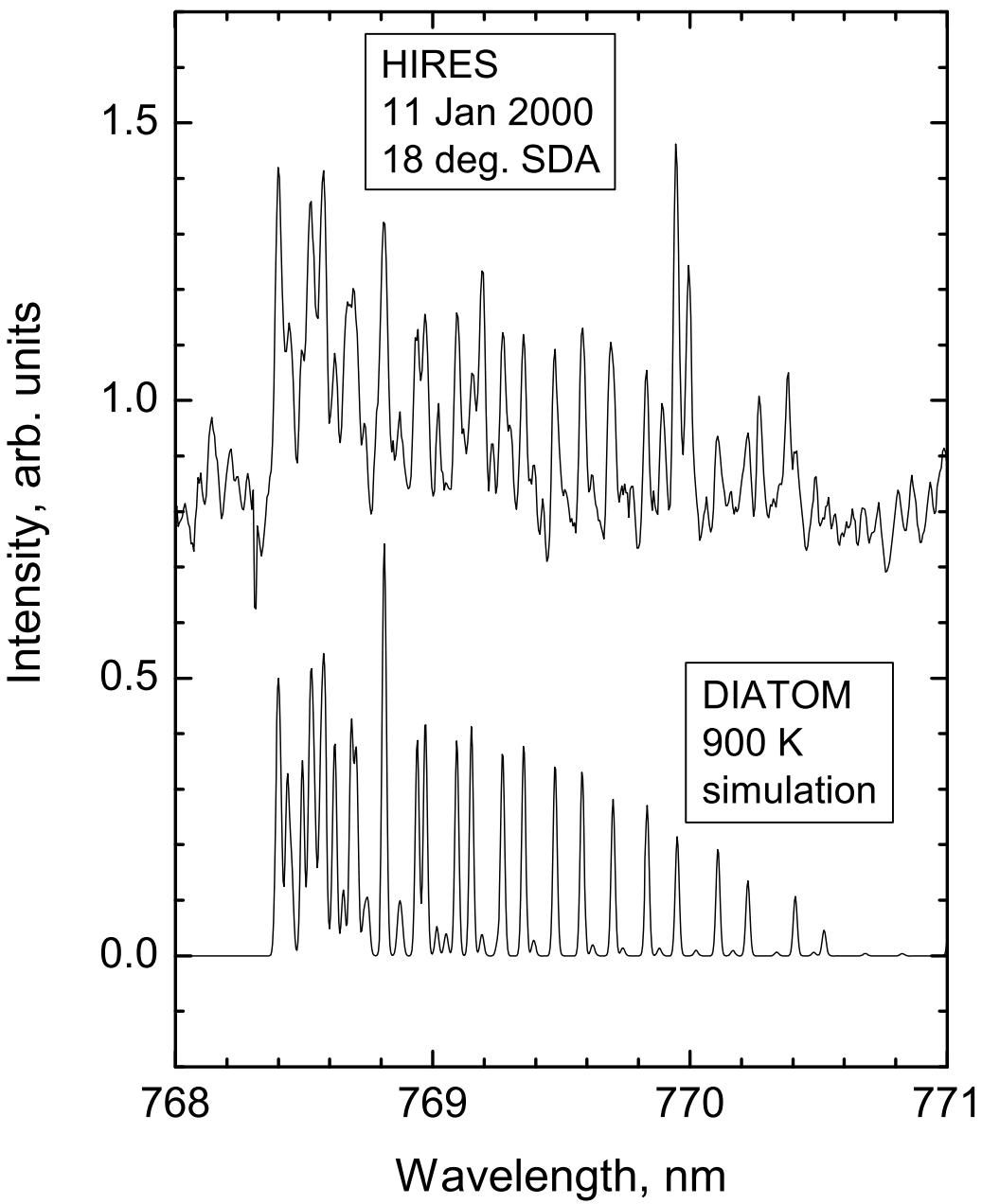
HIRES
11 Jan 2000
18 deg. SDA
DIATOM
900 K
simulation
Intensity, arb. units
Wavelength, nm
0.0
0.5
1.0
1.5
768
769
770
771

Ionospheric $O_2(b)$ Generation

- $O^+ + O_2 \rightarrow O_2^+ + O$
- $O_2^+ + e \rightarrow O(^1D) + O(^3P)$
- $O(^1D) + O_2 \rightarrow O(^3P) + O_2(b, v = 0,1)$
- $O_2(b, v = 1) + O_2 \rightarrow O_2(b, v = 0) + O_2(X, v = 1)$
- Nascent $b(v = 1)/b(v = 0) = 3:1$

Percentage of $O_2(b, v = 1)$ Removed by the three Loss Processes – Radiation, O_2 Quenching, and $O(^3P)$ Quenching – as a Function of Altitude

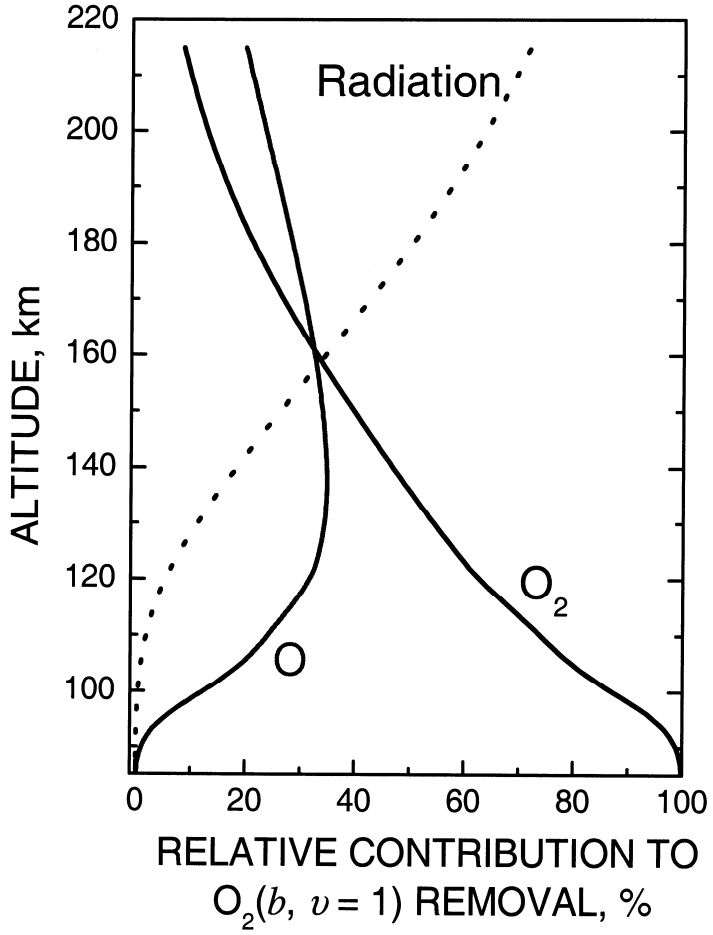

Dayglow spectra in the region of the O_2 Atmospheric 0-0 and 1-1 bands (Arizona GLO experiment on the space shuttle, courtesy of Lyle Broadfoot). The altitude range covered is 142-166 km. The dashed line is a DIATOM simulation of the two bands in the 142 km spectrum, at a resolution of 3 nm and a temperature of 600 K. The modeled intensities are 70:30 (0-0):(1-1).

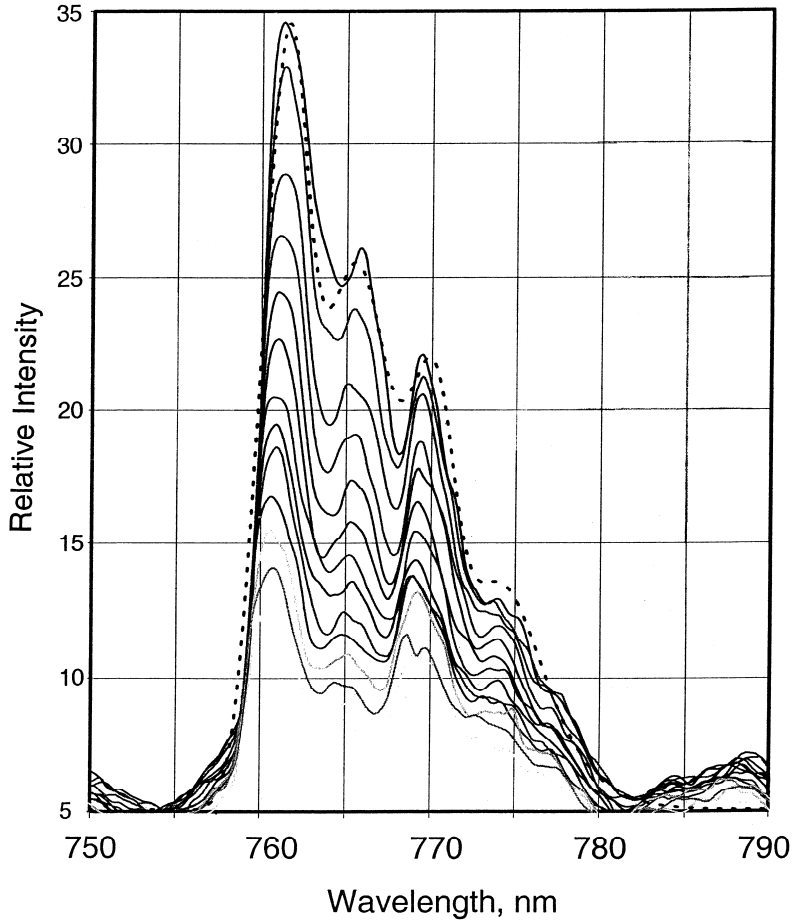

Investigation of $O(^1D) + O(^3P)$

- 1) Photodissociate O_2 at 157 nm; products are $O(^1D) + O(^3P)$
- 2) Use a focused laser beam, so that within a small volume, the O_2 is bleached into atoms.
- 3) Observe the decay of the red line at 630 nm. The only colliders are $O(^3P)$ and $O(^1D)$.
- 4) Vary the laser power and the degree of collisional removal of $O(^1D)$ [with N_2] to separate out the effect of $O(^1D) + O(^1D)$.
- 5) Plot the decay rate against $[O(^3P)]$ (or O_2)

The O(^{1}D) decay rate vs [O(^{3}P)] [*Closser et al.*, 2005].

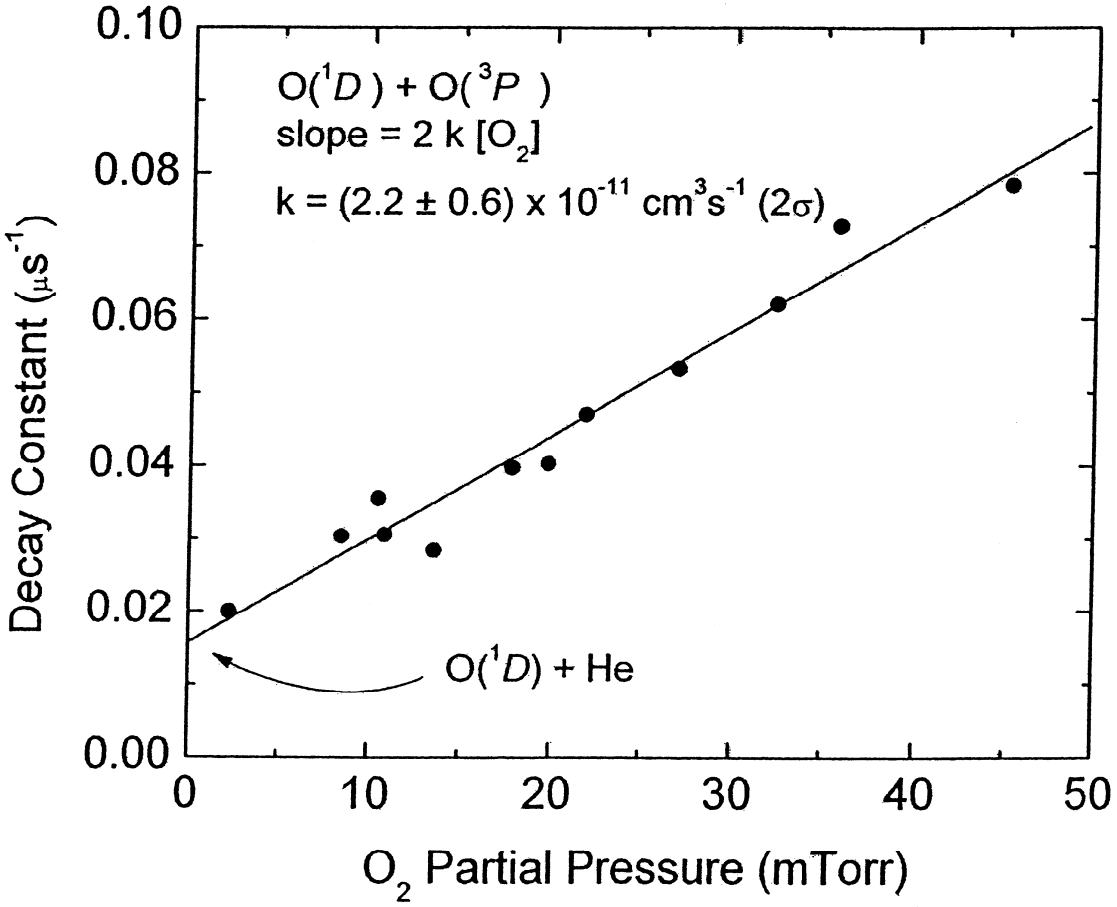

Estimates of the Rate Coefficient for $O(^1D) + O(^3P) \rightarrow O(^3P) + O(^3P)$

Source	Rate coefficient $cm^3\ s^{-1} \times 10^{12}$	Method
Abreu et al. (1986)	8.0 +/- 7.0	calculation
Yee et al. (1990)	6-11 (300 K) 8-13 (1000 K)	calculation
Link and Cogger (1988)	"reaction not required to explain 6300 Å airglow data"	modeling
Sobral et al. (1993)	0-2.8; average - 0.9	atmospheric observation
Slanger (unpublished results, 1985)	20	experiment
Closser et al.. (2005)	22 +/- 6 (300 K)	experiment

O(^{1}D) Decay, Platteville Heater [Sipler and Biondi, 1972]

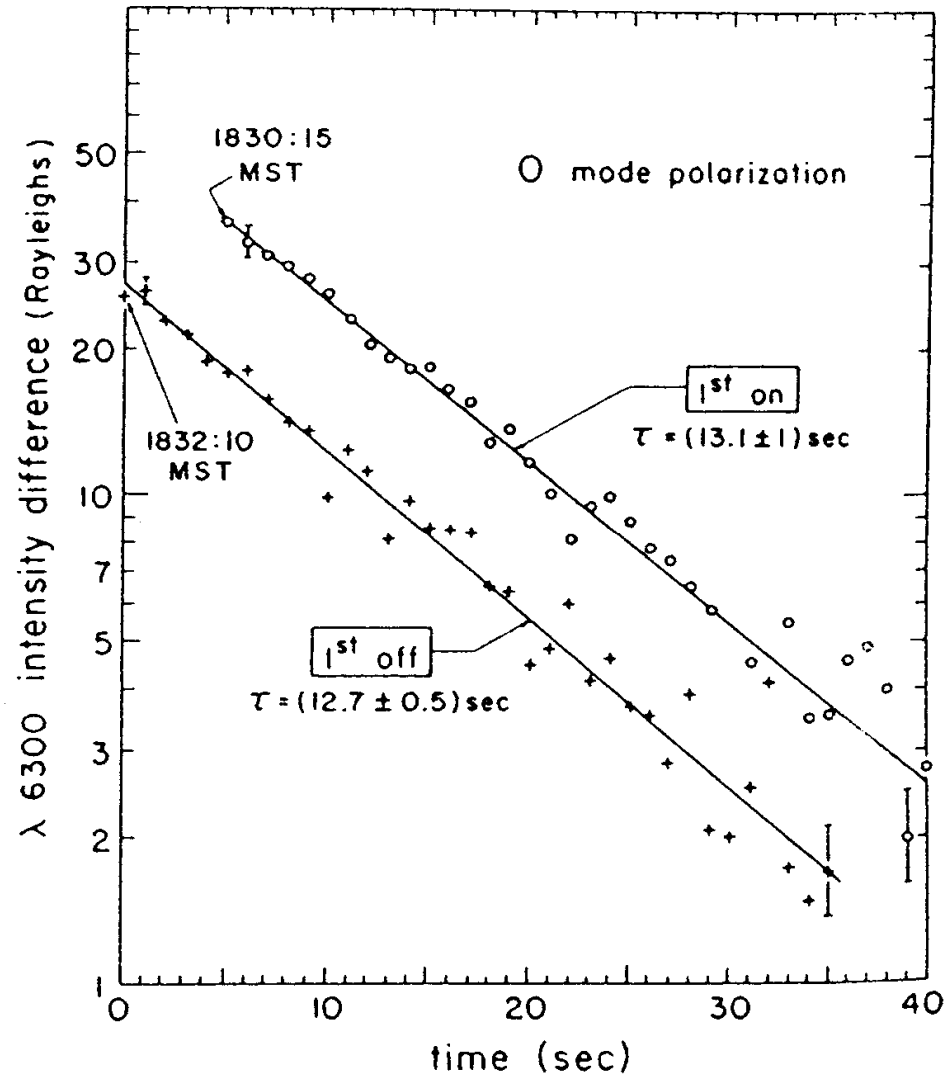

Ionospheric Modification Data for Three Sites, and Comparison of Modeled and Deduced $O(^3P)$ Densities

Site	Date	Source	Lifetime (sec)	Altitude (km)	Deduced $[O(^3P)]$ $cm^{-3} \times 10^{-9}$	MSIS-86 $[O(^3P)]$ $cm^{-3} \times 10^{-9}$
Platteville 49N, 105W	10/30/70 0132 UT	Sipler & Biondi (1972)	12.7 (9.9)	225	2.0	3.06
	10/30/70 0130 UT		13.1 (9.9)	225	1.9	3.06
SURA 56N,46E	3/24/95 1830 UT	Bernhardt et al. (2000)	29.4 (33)	260	0.94	0.77
	3/24/95 1737 UT		43.4 (44)	278	0.54	0.53
HAARP 62N, 145W	3/20/04 0617 UT	Djuth et al. (2005)	54 (44)	290	0.33	0.53

Determination of deduced:modeled $O(^3P)$ and deduced:modeled N_2 for a) $O(^1D)$ collisional loss is primarily due to $O(^3P)$, and b) $O(^1D)$ collisional loss is entirely due to N_2

Site	$[O(^3P)]$ from $O(^1D)$ quenching by $O(^3P)$ Deduced/MSIS	$[N_2]$ (cm^{-3}) Deduced ($\times 10^{-9}$)	$[N_2]$ (cm^{-3}) MSIS-86 ($\times 10^{-9}$)	$[N_2]$ from $O(^1D)$ quenching by N_2 Deduced/MSIS
Platteville	0.65	3.5	1.26	2.8
	0.62	3.4	1.26	2.7
SURA	1.23	1.3	0.21	6.3
	1.03	0.70	0.11	6.5
HAARP	0.62	0.50	0.11	4.6

The fractions of total $O(^1D)$ loss by radiation and the three quenchers – $O(^3P)$, N_2, and O_2 – as a function of altitude.

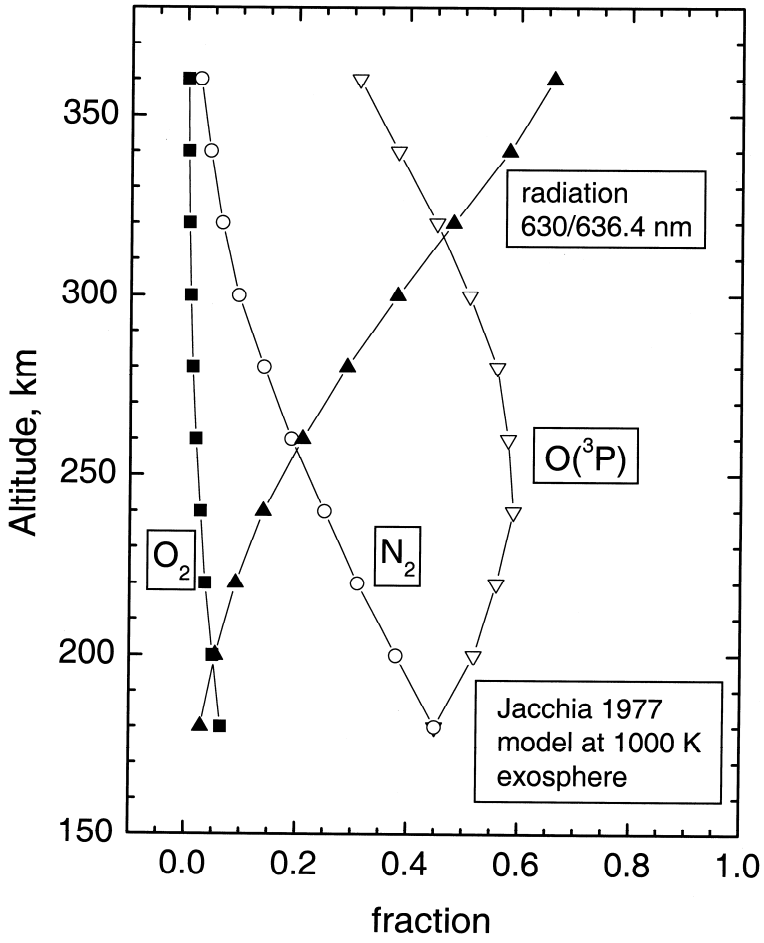

NEEDS

- Measurements of the temperature-dependence of $O(^1D) + O(^3P)$. Yee et al. believe that it is slightly faster at higher temperature.
- Quality red line decay data from the ionospheric heating facilities, over the largest possible range of altitudes.

Conclusions

- At altitudes above ~180 km, oxygen atoms are the most abundant collider. When observing emission from metastable species, which often collide many times before radiating, it is necessary to develop an understanding of the effects of interaction with oxygen atoms.
- We have shown that oxygen red line emission decay is primarily controlled by O-atom collisions, and that it is therefore possible to extract an O-atom density, given the excitation altitude, the decay lifetime, and the (now) known removal rate coefficient.
- Similarly, the ionospheric emission distribution in the related $O_2(b\text{-}X)$ Atmospheric bands can be interpreted in terms of the $[O]/[O_2]$ ratio, so both types of observations can be used for remote sensing of O-atoms.